Journal of Power Sources 240 (2013) 131–139

Contents lists available at SciVerse ScienceDirect

Journal of Power Sources

journal homepage: www.elsevier.com/locate/jpowsour

A high performance polytetrafluoroethene/Nafion composite membrane for vanadium redox flow battery application

Xiangguo Teng*, Jicui Dai, Jing Su, Yongming Zhu, Haiping Liu, Zhiguang Song

School of Marine Science and Technology, Harbin Institute of Technology at Weihai, Weihai 264209, China

HIGHLIGHTS

- A polytetrafluoroethene/Nafion (P/N) membrane for VRB application was prepared.
- The P/N membrane was obtained by impregnating PTFE membrane with Nafion solution.
- The P/N membrane is transparent and flexible with low Nafion resin consumption.
- The P/N membrane has lower vanadium ion permeability and water transport behavior.
- High performances are obtained by using the P/N membrane in VRB single cell tests.

GRAPHICAL ABSTRACT

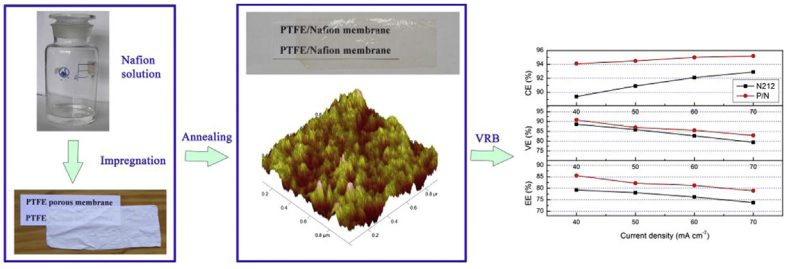

ARTICLE INFO

Article history:
Received 25 January 2013
Received in revised form
13 March 2013
Accepted 30 March 2013
Available online 10 April 2013

Keywords:
Polytetrafluoroethene
Nafion
Vanadium redox flow battery
Membrane

ABSTRACT

To reduce the consumption and improve the performance of Nafion, a thin polytetrafluoroethene (PTFE)/Nafion (P/N) composite membrane for vanadium redox flow battery (VRB) application was prepared by impregnating porous PTFE membrane with Nafion solution. The P/N membrane is almost as transparent as commercial Nafion 212 (N212) membrane, which can be easily cut into any desired shape and size. SEM and AFM analyses prove that the Nafion resin uniformly filled into the micro-pores of porous PTFE membrane. Results also show that the swelling ratio, Nafion consumption, water transport and vanadium ions permeability of P/N membrane are smaller than that of N212. The VRB with P/N membrane has higher coulombic efficiency, voltage efficiency and energy efficiency than that of N212 at all tested current densities, and the average EE of VRB with P/N membrane is 5.2% higher than that of the VRB with N212 at current densities from 40 to 70 mA cm^{-2}. Furthermore, owing to the lower vanadium ions permeability, the self-discharge of the VRB with P/N membrane is much slower than that of the VRB with N212, and 45 cycles charge–discharge test proves that the P/N membrane is very stable and has better capacity retention ability than that of N212.

1. Introduction

All Vanadium redox flow battery (VRB) developed by M. Skyllas-Kazacos and co-workers has been attracted much attention due to its advantages of separated battery capacity, long cycle life, flexible design, high efficiency, quick response time, and environmental friendship [1–3]. Therefore, the VRB is one of the most important and suitable technologies for large-scale renewable and grid energy storage [4,5]. VRB employs an ion exchange membrane as its separator, V(II)/V(III) and V(IV)/V(V) redox couples in sulfuric acid solution as its anolyte and catholyte, respectively. Electrolyte stored

* Corresponding author. Tel./fax: +86 631 5687232.
E-mail address: tengxg0213@yahoo.com.cn (X. Teng).

0378-7753/$ – see front matter © 2013 Elsevier B.V. All rights reserved.
http://dx.doi.org/10.1016/j.jpowsour.2013.03.177

in two tanks is continuously pumped into the stack assembled by carbon bipolar plates [6,7]. With the continuous efforts of the researchers, a series of high performance materials for VRB have been promoted recently. For example, mixed electrolyte (sulfuric and hydrochloric acid), instead of single sulfuric acid, for VRB has shown higher system efficiency, lower capital cost and wider temperature range than that of sulfate electrolyte VRB [8,9]; New type of carbon felt or carbon paper have improved the activity of VRB electrodes [10–12]. Membrane is another key material of VRB system which separates the positive electrolyte and negative electrolyte while still allowing the transport of charge carriers [4]. At present, new and cheaper non-perfluorosulfonated membranes with excellent performance are potential candidates for VRB application [13–16]. However, perfluorosulfonated membrane, such as Nafion is still the most used membrane in VRB for its excellent electrochemical and chemical performances [17]. The limitations of large scale application for Nafion in VRB mainly lie in its low ion selectivity and high cost. To reduce the consumption of Nafion resin, thinner Nafion (<100 μm) membrane with high ion selectivity is much urgently demanded [17]. PTFE/Nafion (P/N) composite membrane has already been successfully developed for fuel cell application. P/N membrane contains much less of the expensive Nafion resin than traditional Nafion 117 (175 μm), Nafion 115 (125 μm) and Nafion 112 (50 μm) membranes [18], and it also can offer good mechanical strength in both swollen and unswollen states, good thermo-stability, easy of handling and availability of very thin membranes [19,21]. Due to the high stability of PTFE membrane, P/N composite membrane can be kept in a stable condition for more than 5000 cycles, about 40% higher than the pure Nafion membrane (about 3500 cycles) [21,22]. Considering that P/N membrane can also be used in VRB, a thickness of 45 μm PTFE/Nafion (P/N) membrane was prepared and tested for VRB application in this paper. The basic chemical–physical properties of the P/N membrane were thoroughly investigated and compared with that of Nafion 212 (N212) membrane, and the VRB single cell performances with P/N membrane were also investigated and compared with that of the VRB with N212 membrane.

2. Experimental

2.1. Materials

Porous PTFE membrane with pore size distribution in the range of 0.3–0.5 μm and porosity 85% was kindly supplied by Xinxiang Xinxing Fenghua Film Factory, Henan Province, China. Nafion solution of 5 wt.% was made according to literature [20]. All the other chemicals were analytic agents and were used as received.

2.2. Membrane preparation

P/N membrane was prepared as described in the literature [18,20]. Briefly, Nafion resin was redissolved in *N*,*N*-dimethylformamide (DMF) to obtain Nafion/DMF solution. PTFE porous membrane was first immersed in 55 °C ethanol for 2 h to facilitate the entry of Nafion solution, then pretreated PTFE film was extended on a clean glass plate. The resulting Nafion/DMF solution was poured onto the treated PTFE film. The impregnated membrane was annealed at 140 °C for 5 h under vacuum and swollen with distilled water until it can be peeled off from the glass plate.

2.3. Membrane characterization

The morphology of the membranes was examined with a field emission environmental scanning electron microscope (Quanta 200F, Czech Republic). The sample surface was coated with gold powder under vacuum before the morphology of membranes was observed. Atomic force microscopy (AFM) was carried out using a Dimension Icon AFM (Bruker, Germany) operated in contact mode. X-ray diffraction (XRD) was measured on a DX2700 diffractometer (Dandong Haoyuan Instrument Co. Ltd., China) using Cu Kα radiation over a 2θ range from 10° to 60°. The dried sample membranes were mounted on an aluminum sample holder.

2.4. Water uptake and swelling ratio

The dry membranes were weighed firstly after they were fully dried under vacuum at 80 °C for 12 h. Then, the sample membranes were immersed in deionized water for another 12 h. Once they were taken out, the excess water on the surface was removed and weighed immediately. The water uptake was calculated according to the following equation:

$$\text{Water uptake}(\%) = \frac{W_w - W_d}{W_d} \times 100\% \quad (1)$$

where W_d and W_w are the weights of the membranes before and after water absorption, respectively.

To evaluate the swelling behavior of the membranes, swelling ratio is denoted as thickness change rate of the membrane. It was calculated by the following equation:

$$\text{Swelling ratio}(\%) = \frac{d_{\text{wet}} - d_{\text{dry}}}{d_{\text{dry}}} \times 100\% \quad (2)$$

where d_{wet} is the thickness of the membrane after being immersed in distilled water for 12 h, and d_{dry} is the thickness of the membranes before water absorption, and the thickness of the samples was measured with a micrometer.

2.5. The ion exchange capacity (IEC)

IEC of the membranes was measured through a titration method. All the samples were dried and weighed before being immersed in a 1.0 mol L^{-1} NaCl solution for 24 h to leach all the H^+ in the membranes. The exchanged H^+ was neutralized with 0.01 mol L^{-1} NaOH solution. The IEC value of the sample membranes was calculated as follows:

$$\text{IEC} = \frac{\Delta V_{\text{NaOH}} \times C_{\text{NaOH}}}{W_{\text{dry}}} \quad (3)$$

where IEC is the desired ion exchange capacity (mmol g^{-1}); ΔV_{NaOH} is the volume of the NaOH used (mL); C_{NaOH} is the concentration of the NaOH (mol L^{-1}), and W_{dry} is the dry weight of the sample membranes (g).

2.6. Proton conductivity

The proton conductivity of the samples was measured by electrochemical impedance spectroscopy (EIS) technique [23] with an IM6e impedance analyzer (Zahner, Germany), the frequency range of 10–10^5 Hz. All the membranes were equilibrated in deionized water for 24 h at room temperature before experiments to ensure that they were completely hydrated.

The conductivity σ (ms cm^{-1}) of the membrane is calculated from the following equation [24]:

$$\sigma = \frac{L}{R \times A} \quad (4)$$

where L (cm) is the distance between two electrodes; R (Ω) is the membrane resistance obtained from the EIS data; A (cm^2) is the cross-sectional area of the membrane.

2.7. Water transport

Water transport was measured according to the literature [25], while a self-made osmotic cell was displayed in Fig. 1. Two half cells were fixed by bolts, a 9.6 cm^2 sample membrane was clamped in the middle, and two glass tubes with calibration marks were used to evaluate the volumetric transfer of the water across the membrane. Volume of 30 mL negative and positive electrolyte under 50% state of charge (SOC) was used on both sides of the cell. The concentration of the electrolyte is 1.5 mol L^{-1} V^{2+}/V^{3+} in 2.5 mol L^{-1} H_2SO_4 solution on one side, and 1.5 mol L^{-1} VO_2^+/VO^{2+} in 2.5 mol L^{-1} H_2SO_4 solution on the other side. The water height in glass tubes on both sides were recorded every 1 h.

2.8. VO^{2+} permeability

The permeability of VO^{2+} was determined according to the literature [26]. Sample membranes with effective area of 1.77 cm^2 were sandwiched between two reservoirs. The left and right reservoirs were filled with 18 mL 1.5 mol L^{-1} $VOSO_4$ and 18 mL 1.5 mol L^{-1} $MgSO_4$ in n mol L^{-1} H_2SO_4 solution ($n = 1.5$, 2.5, 3.5 and 4.5), respectively. Solution in $MgSO_4$ side was periodically taken and measured by a UV–vis spectrometer (Shanghai Jinghua Instruments, China). The absorbance of the samples was measured at a wavelength of 762 nm. The VO^{2+} permeability was calculated by the following equation [27].

$$V_R \frac{dC_R(t)}{dt} = A\frac{P}{L}[C_L - C_R(t)] \quad (5)$$

where C_L is the vanadium ion concentration in the left reservoir; $C_{R(t)}$ is the vanadium ion concentration in the right reservoir as a function of time; t is time; A is the effective area of the samples; L is the thickness of the membrane; P is the permeability of the vanadium ions; and V_R is the volume of right reservoir.

2.9. VRB single cell performance

A VRB single cell was built by sandwiching the membrane between two pieces of 5 mm graphite felt electrodes. Two graphite polar plates were used as current collectors, and the effective reaction area of membrane and electrodes were 9 cm^2. The catholyte was 40 mL of 1.5 mol L^{-1} V(IV) in 2.5 mol L^{-1} H_2SO_4 solution; and the anolyte was 1.5 mol L^{-1} V(III) in 2.5 mol L^{-1} H_2SO_4 solution.

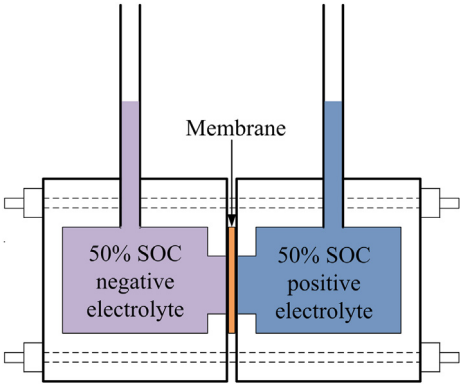

Fig. 1. Osmotic cell used for determination of water transport behavior through different membranes.

The cutoff voltages for the test were 1.65 V and 0.8 V to avoid the corrosion of graphite. Charge–discharge of the cell was controlled by a land CT2001C (Wuhan Land Electronics Co., Ltd., China) battery instrument. The coulombic efficiency (CE), voltage efficiency (VE), and energy efficiency (EE) of the VRB single cell were calculated according the following equations as used in literature [6].

$$CE = \frac{\text{discharge capacity}}{\text{charge capacity}} \times 100\% \quad (6)$$

$$VE = \frac{\text{middle point of discharge voltage}}{\text{middle point of charge voltage}} \times 100\% \quad (7)$$

$$EE = CE \times VE \quad (8)$$

3. Results and discussion

3.1. Consumption of Nafion

Because the thickness of N212 (50 μm) is very similar to that of prepared P/N membrane (45 μm), N212 is chosen for control experiments. Based on the calculation, the N212 membrane weight is 0.0101 g per square centimeter; while for P/N membrane, the weight of Nafion resin consumed is 0.0075 g per square centimeter. Compared with N212, the Nafion resin consumption for P/N membrane has decreased 25.7%. Consequently, the cost will be dramatically decreased if the P/N membrane can be used for VRB application.

3.2. Membrane morphology

Different from the porous PTFE membrane, the P/N membrane is very similar to commercial N12 membrane, which is transparent, flexible and can be easily cut into any shape and size, which can be seen in Fig. 2. According to the reported literature [18], there are micro-pores formed by fibers with knots on the surface of porous PTFE membrane. However, from Fig. 2, it can be seen that the

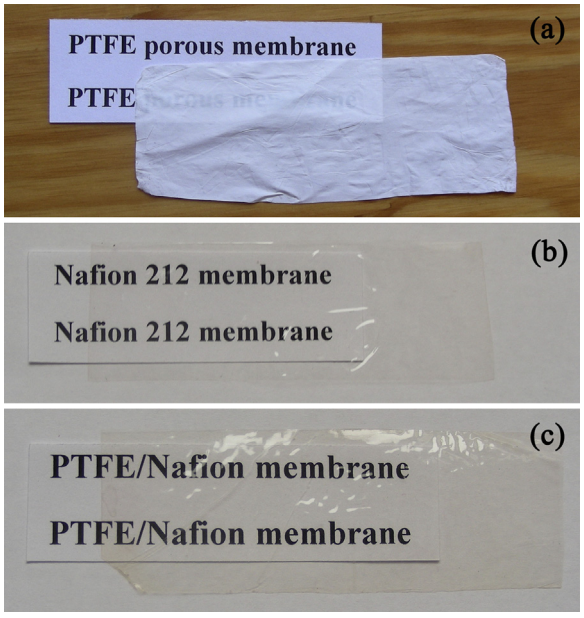

Fig. 2. Photographs of PTFE porous membrane (a), N212 membrane (b) and P/N membrane (c) (Taken by a Nikon COOLPIX camera).

appearance of P/N membrane are almost the same as N212 membrane. SEM images (Fig. 3) were further taken to compare the difference between N212 and P/N membranes. Fig. 3 shows that the surface of P/N membrane is compact and smooth, which further proves that no micro-pores are observed and all micro-pores in PTFE membrane should be filled and covered with Nafion resin. The result is similar to the studies of literature [19,20]. Therefore, it can be concluded that Nafion resin is distributed uniformly in the P/N membrane and completely impregnated in the micro-pores of the PTFE membrane.

Topography difference between the P/N and N212 membranes were also detected by AFM method and the three-dimensional images were illustrated in Fig. 4. As can be seen, the distribution of the topographic for both P/N and N212 membranes is rough and irregular. It can also be observed that the peak-valley differences of P/N membrane are not as obvious as that of N212 membrane, which means the surface of the P/N membrane is smoother than that of N212 membrane. Based on the AFM image, the maximum vertical distance between the highest and lowest data points is 4.51 nm and 8.36 nm for P/N and N212 membranes, respectively. Furthermore, surface area difference of P/N and N212 membranes is 0.193% and 0.346%, respectively. From these results, it can be concluded that the surface of the P/N membrane is more uniform than that of N212 membrane.

3.3. X-ray diffraction

Fig. 5 shows the X-ray diffraction (XRD) patterns of native PTFE, N212 and P/N membrane. It can be seen that pure PTFE membrane shows a sharp scattering peak at $2\theta = 18^\circ$, which is well in accordance with the standard XRD pattern of PTFE (PDF# 00-054-1594). For N212 membrane, two broad scattering peaks at $2\theta = 12-20^\circ$ and $2\theta = 40^\circ$ can be observed, which is due to the amorphous ($2\theta = 16^\circ$, 40°) and crystalline ($2\theta = 17.5^\circ$) part in Nafion [28–30]. For the P/N membrane, weak broad scattering peak at $2\theta = 40^\circ$, weak scattering peak at $2\theta = 17.5^\circ$ and a sharp scattering peak at $2\theta = 18^\circ$ indicate that the XRD pattern of P/N membrane is the combination of N212 and PTFE membranes. Furthermore, it can also be noted that the characteristic scattering peaks of Nafion in P/N membrane are very weak, which indicates that the Nafion content is relatively lower in the composite membrane.

3.4. Chemical–physical properties of the developed membrane

Water is important to Nafion, however, an excess of absorbed water can also lead to exaggerated swelling and decrease the ion selectivity as well as destroying the mechanical properties of the membrane [31]. From Table 1, it can be seen that the water uptake and swelling ratio of P/N membrane are all smaller than that of N212 membrane. The reason can be attributed to that PTFE membrane is high hydrophobic which can efficiently suppress the swelling and decrease the water absorption of Nafion [20]. As a result, the water uptake and swelling ratio of P/N membrane decreased 19.5% and 33.8% compared to that of N212. Furthermore, although PTFE has high mechanical stability and chemical stability, it is non proton conductor which consequently decreased the IEC and conductivity of P/N membrane compared with bare N212 membrane.

3.5. Water transport behavior

During the charge–discharge process of VRB, several reasons can lead to the preferential volumetric water transfer across the membrane and lead to a reduction in the cell capacity as well as possible flooding of the solution reservoir [32]. Therefore, one of the most important requirements for a membrane used in VRB is that it can prevent excessive transfer of water from one half cell to the other [33]. In this work, the water transfer properties of P/N and N212 membranes were measured and displayed in Fig. 6. It can be observed that the net water transfer for both P/N and N212 membranes is from negative electrolyte cell to positive electrolyte cell, which is in agree with the previous results [32–34]. Furthermore, the volume change of water across the P/N and N212 membranes during whole test time is 0.43 mL (30 h $cm^2)^{-1}$ and 0.36 mL (30 h $cm^2)^{-1}$, respectively. Consequently, by using P/N membrane, the water transfer rate has been decreased 16.3% compared to that of N212 membrane. From the results, it can be expected that the P/N membrane can effectively minimize the water transfer between negative and positive electrolyte in VRB. As mentioned above, several processes are responsible for the water transfer in VRB during charge–discharge cycling in VRB. Whereas, higher IEC is one of the reasons that can possibly increase the water transfer across the membrane [34]. In this experiment, the IEC of P/N membrane is lower than that of N212 membrane. As a result, water suppression ability of P/N membrane is superior to that of N212 membrane.

3.6. VO^{2+} permeability

It is essential that a membrane used in VRB should possess low vanadium ions permeability to increase the coulombic efficiency and decrease the self-discharge of the cell. On the other hand, due to the solubility of $VOSO_4$ decreases with increasing H_2SO_4

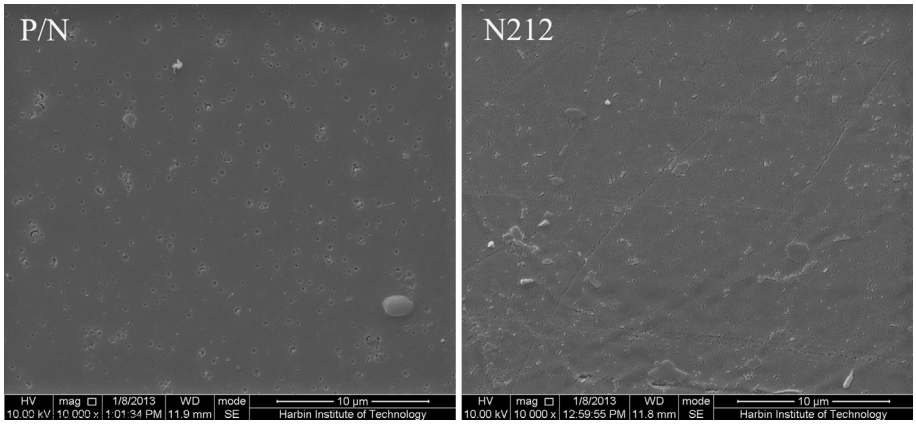

Fig. 3. SEM micrographs of P/N and N212 membranes.

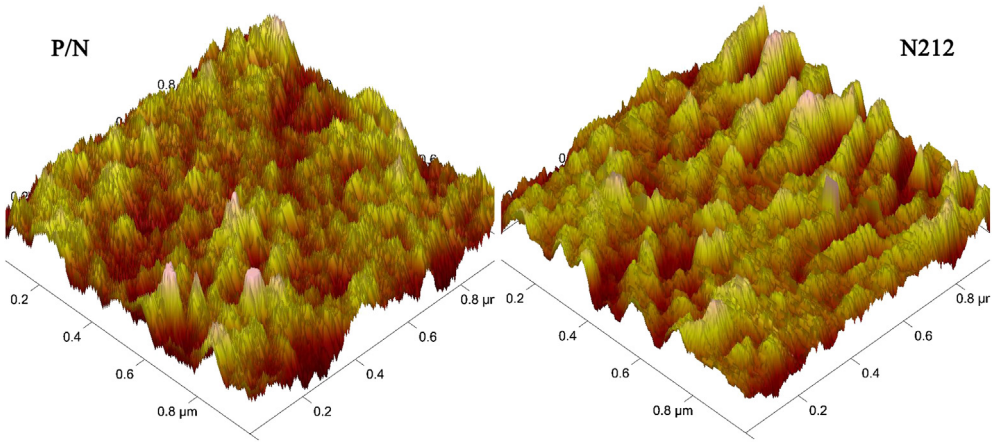

Fig. 4. Three dimensional AFM images of P/N and N212 membranes.

concentration, the concentration of total SO_4^{2-} in the VRB electrolyte is usually controlled at less than 5 mol L^{-1} [4]. Therefore, to investigate the performance of P/N membrane in VRB electrolyte, the change of VO^{2+} concentration *versus* diffuse time in 1.5, 2.5, 3.5 and 4.5 mol L^{-1} H_2SO_4 solutions with P/N and N212 membranes are analyzed as shown in Fig. 7. It can be seen that the concentration of VO^{2+} increased linearly with time for P/N membrane as well as N212 membrane in all tested electrolyte, and the VO^{2+} concentration across P/N membrane is all smaller than that of N212 at the same diffusion time. VO^{2+} permeability of P/N and N212 membranes is calculated and shown in Fig. 8. The VO^{2+} permeability values of P/N membrane are between 1.09×10^{-8} cm^2 min^{-1} (in 4.5 mol L^{-1} H_2SO_4) and 4.62×10^{-8} cm^2 min^{-1} (in 1.5 mol L^{-1} H_2SO_4); while for N212 membrane, the VO^{2+} permeability values are between 2.80×10^{-8} cm^2 min^{-1} (in 4.5 mol L^{-1} H_2SO_4) and 6.67×10^{-8} cm^2 min^{-1} (in 1.5 mol L^{-1} H_2SO_4). Compared to that of N212 membrane in the H_2SO_4 concentration of 1.5 mol L^{-1}, 2.5 mol L^{-1}, 3.5 mol L^{-1} and 4.5 mol L^{-1}, the permeability of P/N membrane is 69.3%, 70.1%, 50.0% and 38.9%, respectively. This result clearly shows that the VO^{2+} suppression ability of P/N membrane is superior to that of N212 membrane. As can be expected, the VRB with P/N membrane will have higher coulombic efficiency and lower self discharge rate due to its lower VO^{2+} permeability, which can be proved by the experiments in the next section. It can also be seen from Fig. 8 that the VO^{2+} permeability of both P/N membrane and N212 membranes in higher concentration H_2SO_4 solution is smaller than that of in lower concentration H_2SO_4 solution. The reason can be due to the lower VO^{2+} diffusion velocity in higher concentration H_2SO_4 solution with higher viscosity [35]. Another reason may be that as H_2SO_4 concentration increases, the ion exclusion effect between VO^{2+} and H^+ is strengthened and thus blocks the diffusion of VO^{2+}. Furthermore, the appearance of the P/N membrane has no change in all concentration of H_2SO_4 solution, indicating that the P/N membrane is very stable.

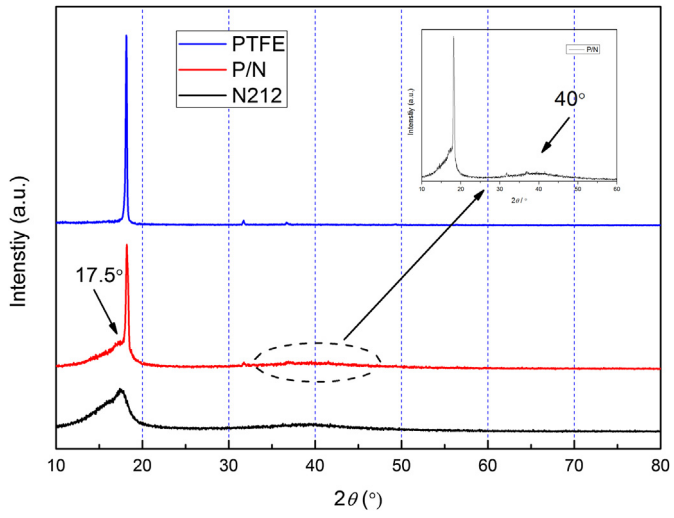

Fig. 5. XRD patterns of PTFE, P/N and N212 membranes.

3.7. VRB single cell performance

Charge–discharge curves of the VRB with P/N and N212 membranes at current density of 40–70 mA cm^{-2} are shown in Fig. 9. It can be seen that the discharge capacities of the VRB with P/N membrane are all higher than that of the VRB with N212 membrane at all current densities, which proves that P/N membrane has excellent performance to restrain the crossover of vanadium ion than that of N212 membrane. From Fig. 9, it can also be observed that the discharge voltages of the VRB with P/N membrane are all higher than that of the VRB with N212 membrane, which indicates that the inner resistance of the VRB with N212 is higher than that of the VRB with P/N membrane. Detailed relationship between the CE, VE, and EE with charge–discharge current densities of the VRBs with P/N and N212 membranes is illustrated in Fig. 10. As shown in Fig. 10, the CEs of VRB with N212 and P/N membranes all increase with current density, which can be due to the shorter permeation time for vanadium ions at higher current density. The VEs of two VRBs both decrease with current density, which is because of the higher ohmic polarization at higher current density of the cell [14]. The EEs for both VRBs decrease with current density because of the decrease rate of VEs is higher than that of CEs. Furthermore, the CEs, VEs and EEs of VRB with P/N membrane are all higher than that of the VRB with N212 membrane. The higher CEs of the VRB with P/N membrane can be owing to the existence of PTFE matrix in the composite membrane which decreases the effective permeability channels for VO^{2+} to pass through. The reason for higher VEs of the

Table 1
Comparison of chemical–physical properties of P/N with N212 membrane.

Membrane	Thickness (μm, dried)	Water uptake (%)	Swelling ratio (%)	IEC (mmol g^{-1})	Conductivity (mS cm^{-1})
N212	50	30.8	15.1	0.88	72.4
P/N	45	24.9	10.0	0.69	68.1

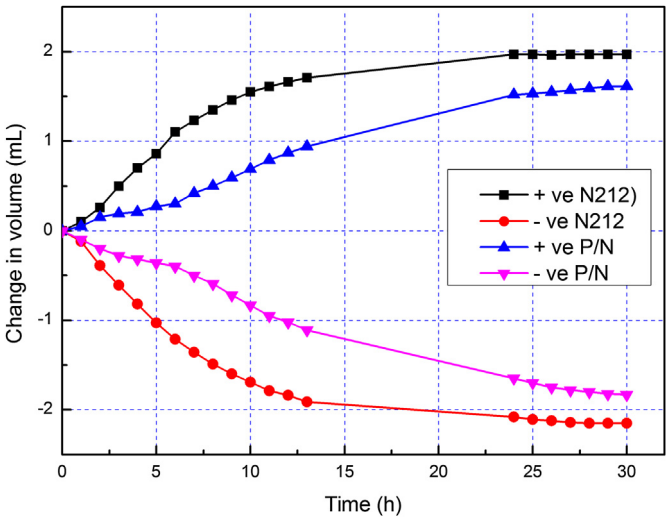

Fig. 6. Water transfer behavior of P/N and N212 membranes.

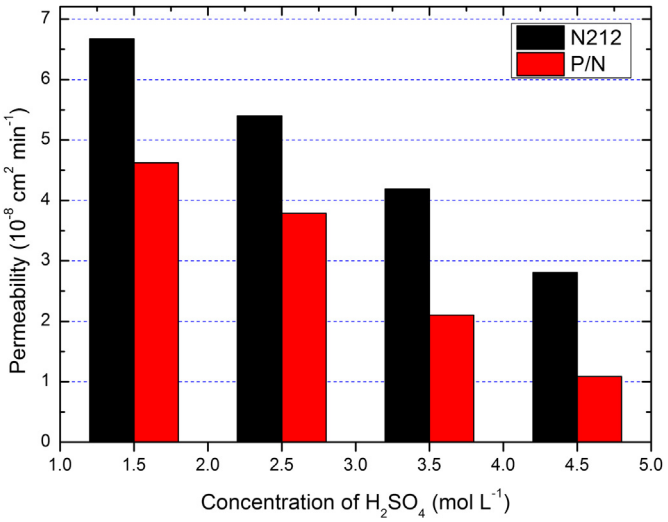

Fig. 8. VO^{2+} permeability of P/N and N212 membranes in different concentration of H_2SO_4 solution.

P/N membrane based VRB lies in its thinner layer than that of N212 membrane, and thus the VRB with P/N membrane has lower ohmic polarization. Consequently, the EEs of VRB with P/N membrane have the higher values than that of N212 based VRB at all tested current densities. The highest EE of VRB with P/N and N212 membrane is 85.5% and 79.2% at current density of 40 mA cm^{-2}, respectively; and the average EE of VRB with P/N membrane is 5.2% higher than that of the VRB with N212 membrane at current densities from 40 to 70 mA cm^{-2}. It should also be noted that the EE of the VRB with N212 membrane in this experiment (78.1%) at current density of 50 mA cm^{-2} is much lower than the result reported by Chen et al. (about 91.5%) [36]. But the result is higher than the value reported by Chen et al. (about 73%) [14], and it agrees with the value reported by Jia et al. (about 78%) [37] and Ling et al. (78%) [38]. The reason should be due to the different materials such as electrode, electrolyte, collector; assembly techniques or instruments used in the different laboratories.

The open circuit voltage (OCV) can be used to illustrate the self-discharge of a VRB, which is mainly caused by the crossover of vanadium ions across the membrane between the catholyte and anolyte. In this work, the OCV of VRBs with P/N and N212 membranes was measured and recorded after it was charged to a 50% state and illustrated in Fig. 11. As can be found from Fig. 11, the OCV value of both VRBs gradually decrease with measured time firstly, and then dramatically reduce at about 1.25 V. It can also be seen that the time of OCV keeping at above 0.8 V for VRB with the P/N membrane is beyond 140 h, which is 2.4 times longer than that of

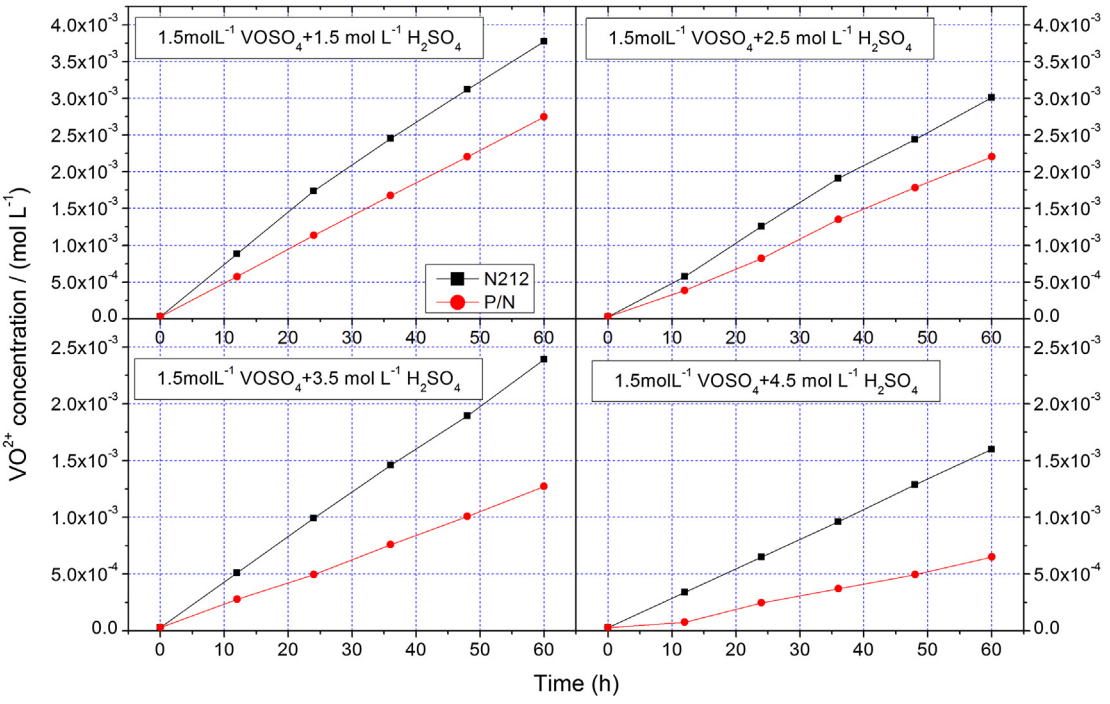

Fig. 7. VO^{2+} concentration varied with diffusion time based on P/N and N212 membranes in different concentration of H_2SO_4 solution.

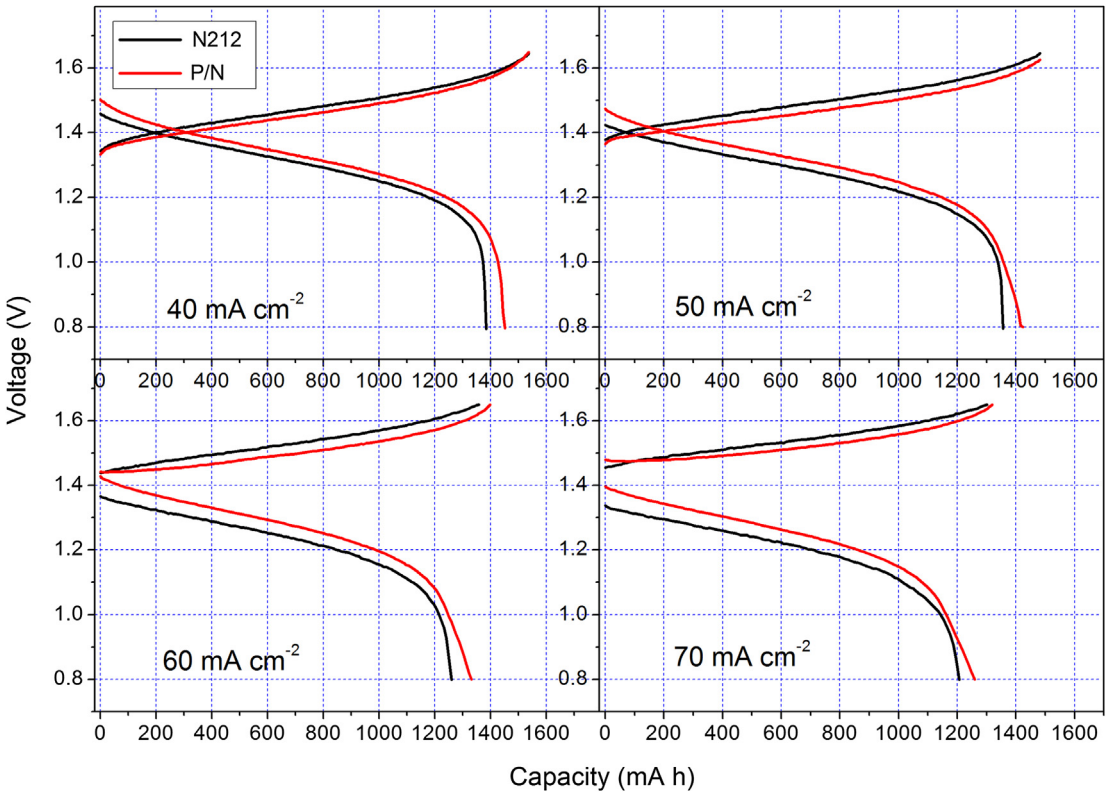

Fig. 9. Charge–discharge curves of VRBs with P/N and N212 membranes at various current densities.

VRB with N212 membrane. The result reveals that the self-discharge of VRB with P/N membrane is much slower than that of the VRB with N212 membrane, which can be due to the lower vanadium ion permeability of P/N membrane as proved in VO^{2+} permeability experiment.

To further investigate the stability of the membrane, the cycling performances of VRB employing P/N and N212 membranes tested at current density of 80 mA cm^{-2} are presented in Fig. 12. It can be observed that the CEs of the VRB with both P/N and N212 membranes are stable and remain almost constant after being charge–discharged for 45 cycles. Although the VEs of the VRB with both P/N and N212 membranes decline slowly with the cycle numbers, the VE decline rate of the VRB with P/N membrane is much slower than that of the VRB with N212 membrane. As a result, the EEs of the VRB with P/N membrane are much higher and decline much slower than that of the VRB with N212 membrane during the whole cycle life test. This result further proves that the P/N membrane possesses good chemical stability and high cell performances in strong acidic vanadium solutions. It should also be pointed out that the CE difference between the VRB with P/N and N212 membranes is rather smaller than the VE difference between two cells. The reason is due to the shorter permeation time for vanadium ions and lower

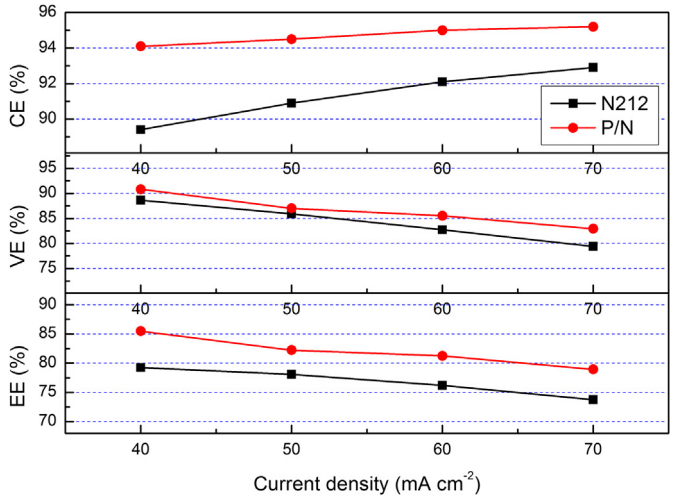

Fig. 10. Relationship between CE, VE and EE with the current density of the VRBs with P/N and N212 membranes.

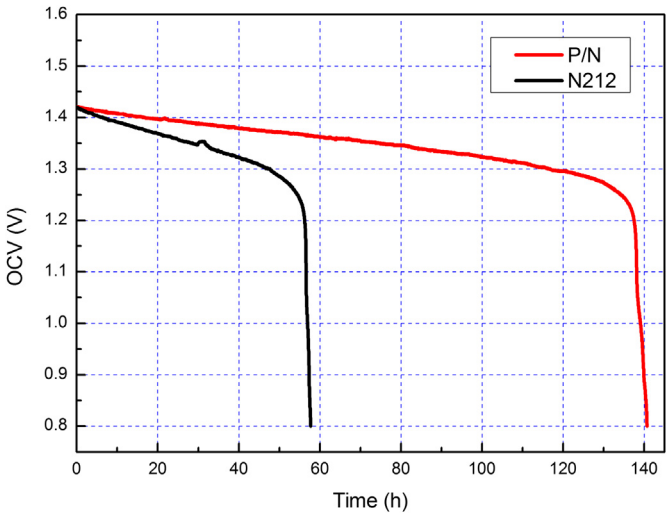

Fig. 11. OCV of the VRBs with P/N and N212 membranes at a SOC of 50%.

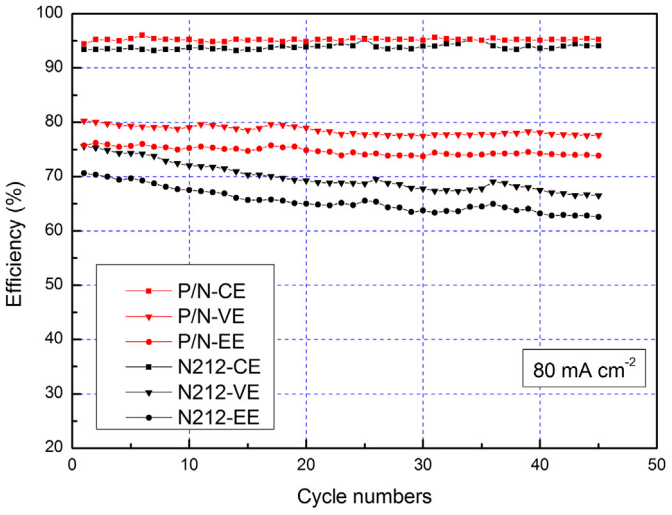

Fig. 12. Cycling performance of efficiencies for VRBs with P/N and N212 membranes at 80 mA cm^{-2}.

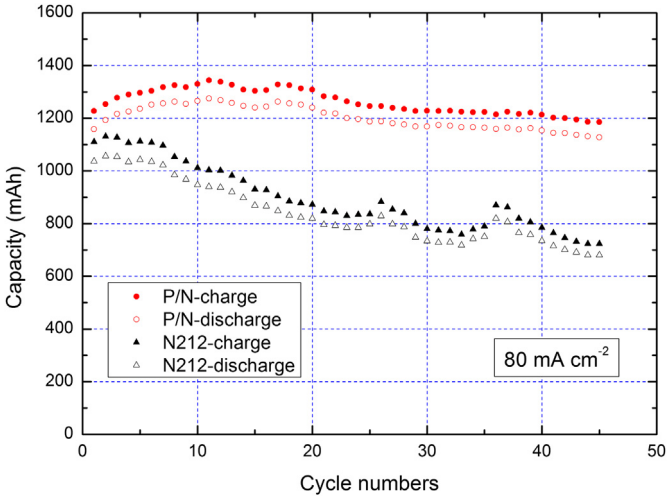

Fig. 13. Charge–discharge capacity decay of VRBs with P/N and N212 membranes corresponding to Fig. 12.

ohmic polarization of the VRB with P/N membrane at higher current density. Furthermore, the lower ohmic polarization and vanadium ion permeability of the P/N membrane also helps to improve the charge and discharge capacity as shown in Fig. 13. It is obvious that both the charge and discharge capacities of the VRB with P/N membrane are much higher than that of the VRB with N212 membrane. After 45 cycles, the charge and discharge capacity of the VRB with P/N membrane has almost no loss, while for the VRB with N212 membrane, both the charge and discharge capacity is only about 65.6% of its initial capacity.

4. Conclusions

A 45 μm PTFE/Nafion membrane based on porous PTFE membrane with high battery performance was prepared. SEM and AFM analyses showed that the surface of porous PTFE has been uniformly covered by Nafion resin. Owing to the hydrophobic nature of porous PTFE, P/N membrane showed lower water uptake, IEC, swelling ration and conductivity than that of N212 membrane. But the P/N membrane showed lower water transfer behavior and vanadium ions permeability than that of the N212 membrane due to its thinner layer and low IEC. As a result, the coulombic efficiency, voltage efficiency and energy efficiency of the VRB with P/N membrane were all higher than that of N212 membrane at all tested current densities. Self-discharge of the VRB with P/N membrane was also much lower than that of the VRB with N212 membrane. Furthermore, the VRB employing P/N membrane has good cycling performances and better capacity retention ability than that of the VRB with N212 membrane. All results indicate that the P/N membrane is very promising to be used in VRB to reduce the consumption and improve the performance of currently used Nafion membrane.

Acknowledgments

This work was funded by Natural Scientific Research Innovation Foundation in Harbin Institute of Technology (HIT. NSRIF. 2011107). The authors thank Mr. Jie Yu for the SEM and Miss Lin Yang for AFM analysis of the samples. The authors greatly thank Professor C. Gao and L. Cao for language improvements on the original version of this manuscript.

References

[1] M. Skyllas-Kazacos, M. Rychcik, R.G. Robins, A.G. Fane, M.A. Green, Journal of the Electrochemical Society 133 (1986) 1057–1058.
[2] M. Skyllas-Kazacos, D. Kasherman, D.R. Hong, M. Kazacos, Journal of Power Sources 35 (1991) 399–404.
[3] C. Gao, N. Wang, S. Peng, S. Liu, Y. Lei, X. Liang, S. Zeng, H. Zi, Electrochimica Acta 88 (2013) 193–202.
[4] Z. Yang, J. Zhang, M.C.W. Kintner-Meyer, X. Lu, D. Choi, J.P. Lemmon, J. Liu, Chemical Reviews 111 (2011) 3577–3613.
[5] W. Wang, Q. Luo, B. Li, X. Wei, L. Li, Z. Yang, Advanced Functional Materials 23 (2013) 970–986.
[6] J.Y. Xi, Z.H. Wu, X.G. Teng, Y.T. Zhao, L.Q. Chen, X.P. Qiu, Journal of Materials Chemistry 18 (2008) 1232–1238.
[7] D. Chen, S. Wang, M. Xiao, Y. Meng, Journal of Power Sources 195 (2010) 2089–2095.
[8] L. Li, S. Kim, W. Wang, M. Vijayakumar, Z. Nie, B. Chen, J. Zhang, G. Xia, J. Hu, G. Graff, J. Liu, Z. Yang, Advanced Energy Materials 1 (2011) 394–400.
[9] S. Kim, E. Thomsen, G. Xia, Z. Nie, J. Bao, K. Recknagle, W. Wang, V. Viswanathan, Q. Luo, X. Wei, A. Crawford, G. Coffey, G. Maupin, V. Sprenkle, Journal of Power Sources 237 (2013) 300–309.
[10] W. Zhang, J. Xi, Z. Li, H. Zhou, L. Liu, Z. Wu, X. Qiu, Electrochimica Acta 89 (2013) 429–435.
[11] K.J. Kim, M. Park, J. Kim, U. Hwang, N.J. Lee, G. Jeong, Y. Kim, Chemical Communications 48 (2012) 5455–5457.
[12] M.P. Manahan, Q.H. Liu, M.L. Gross, M.M. Mench, Journal of Power Sources 222 (2013) 498–502.
[13] N. Wang, S. Peng, H. Wang, Y. Li, S. Liu, Y. Liu, Electrochemistry Communications 17 (2012) 30–33.
[14] D. Chen, M.A. Hickner, E. Agar, E.C. Kumbur, Electrochemistry Communications 26 (2013) 37–40.
[15] H. Zhang, H. Zhang, X. Li, Z. Mai, J. Zhang, Energy & Environmental Science 4 (2011) 1676–1679.
[16] W. Wei, H. Zhang, X. Li, Z. Mai, H. Zhang, Journal of Power Sources 208 (2012) 421–425.
[17] X. Li, H. Zhang, Z. Mai, H. Zhang, I. Vankelecom, Energy & Environmental Science 4 (2011) 1147–1160.
[18] T.L. Yu, H.L. Lin, K.S. Shen, L.N. Huang, Y.C. Chang, G.B. Jung, J.C. Huang, Journal of Polymer Research 11 (2004) 217–224.
[19] H. Lin, T.L. Yu, L. Huang, L. Chen, K. Shen, G. Jung, Journal of Power Sources 150 (2005) 11–19.
[20] F. Liu, B. Yi, D. Xing, J. Yu, H. Zhang, Journal of Membrane Science 212 (2003) 213–223.
[21] H.L. Tang, M. Pan, F. Wang, Journal of Applied Polymer Science 109 (2008) 2671–2678.
[22] T. Jao, G. Jung, P. Chi, S. Ke, S. Chan, Journal of Power Sources 196 (2011) 1818–1825.
[23] T.A. Zawodzinski, M. Neeman, L.O. Sillerud, S. Gottesfeld, The Journal of Physical Chemistry 95 (1991) 6040–6044.
[24] B. Qiu, B. Lin, L. Qiu, F. Yan, Journal of Materials Chemistry 22 (2012) 1040–1045.
[25] T. Mohammadi, S.C. Chieng, M.S. Kazacos, Journal of Membrane Science 133 (1997) 151–159.
[26] F. Grossmith, P. Liewellyn, A.G. Fane, M. Skyllas-Kazacos, in: Proc. Electrochem. Soc. Symp., Honolulu (1988), p. 363.

[27] X.L. Luo, Z.Z. Lu, J.Y. Xi, Z.H. Wu, W.T. Zhu, L.Q. Chen, X.P. Qiu, Journal of Physical Chemistry B 109 (2005) 20310–20314.
[28] W. Xu, T. Lu, C. Liu, W. Xing, Electrochimica Acta 50 (2005) 3280–3285.
[29] Z. Chen, B. Holmberg, W. Li, X. Wang, W. Deng, R. Munoz, Yan, Chemistry of Materials 18 (2006) 5669–5675.
[30] P. Staiti, A.S. Aricò, V. Baglio, F. Lufrano, E. Passalacqua, V. Antonucci, Solid State Ionics 145 (2001) 101–107.
[31] D.Y. Chen, S.J. Wang, M. Xiao, Y.Z. Meng, Energy & Environmental Science 3 (2010) 622–628.
[32] T. Mohammadi, M. Skyllaskazacos, Journal of Power Sources 56 (1995) 91–96.
[33] Q.T. Luo, H.M. Zhang, J. Chen, P. Qian, Y.F. Zhai, Journal of Membrane Science 311 (2008) 98–103.
[34] T. Mohammadi, M.S. Kazacos, Journal of Power Sources 63 (1996) 179–186.
[35] F.H. Rhodes, C.B. Barbour, Industrial & Engineering Chemistry 15 (1923) 850–852.
[36] D. Chen, S. Kim, L. Li, G. Yang, M.A. Hickner, RSC Advances 2 (2012) 8087–8094.
[37] C. Jia, J. Liu, C. Yan, Journal of Power Sources 203 (2012) 190–194.
[38] X. Ling, C. Jia, J. Liu, C. Yan, Journal of Membrane Science 415–416 (2012) 306–312.